Estimating Inelastic Drifts and Link Rotation Demands in EBFs

PAUL W. RICHARDS and BRANDON THOMPSON

The ductility of steel eccentrically braced frames (EBFs) depends on stable inelastic rotation of the links (Roeder and Popov, 1978). Experimental testing of ASTM A992 links has shown that well-stiffened shear-yielding links can accommodate large inelastic rotations without significant loss of strength (Okazaki et al., 2005). Current provisions require designers to detail links with appropriate stiffeners depending on the expected inelastic rotation demands (AISC, 2005). EBFs are unique, when compared to other ductile braced frames or special moment resisting frames, in that specific detailing (the link stiffener spacing) is directly related to the estimated inelastic deformation.

Typically, a designer will amplify elastic analysis results to estimate EBF link inelastic rotations. First, the displacements and story drifts are obtained from a static elastic analysis of the EBF under the equivalent lateral force. Next, elastic story drifts are multiplied by a deformation amplification factor, C_d, to estimate the inelastic story drifts (ICC, 2006). Finally, with the estimated inelastic story drifts, the designer estimates link inelastic rotations using simplified rigid-plastic relationships (Figure 1, for example).

Two issues may limit the accuracy of the practice just described. First, the definition of story drift in the provisions (ICC 2006) includes components from column deformations that are likely unrelated to link demands. Second, the deformation amplification factor, even if reasonable for computing inelastic roof drifts, may not be reasonable for computing inelastic story drifts. The first issue is discussed in the following paragraph, while the second is discussed in the following section.

It may be unreasonable to amplify the total elastic story drift by C_d to estimate the inelastic story drift in tall frames. Provisions define story drift as the relative lateral displacement of the top and bottom of a story, divided by the story height (ICC, 2006). When columns of a particular story experience axial deformation, frame "flexural" deformation increases story drifts for all stories above (see Figure 2, left). In contrast, brace and beam deformations at a particular story cause frame "shear" deformation and do not impact story drifts beyond that story (Figure 2, middle). The total story drift is greatest in the upper stories of tall frames because of frame flexural deformation. Therefore, link inelastic rotations will always be predicted to be greatest in the top stories of tall frames. Some engineers consider it overly conservative to amplify total elastic story drifts by C_d because inelastic story drifts (and link rotations) are related only to frame shear distortions (Horne et al., 1999).

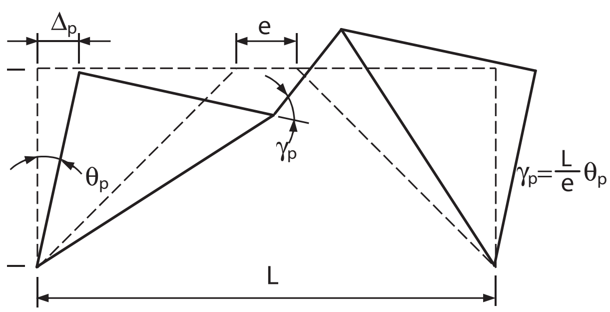

Fig. 1. Relationship between inelastic story drift and inelastic link rotation (AISC, 2005).

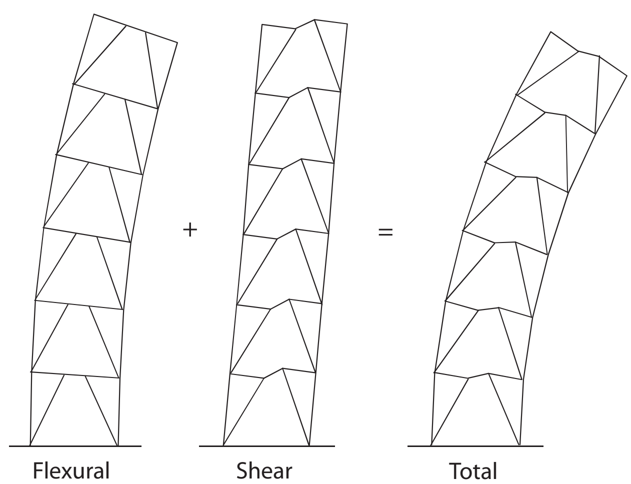

Fig. 2. Components of story and frame deformation.

Paul W. Richards is an assistant professor in the department of civil and environmental engineering, Brigham Young University, Provo, UT.

Brandon Thompson is a graduate student researcher in the department of civil and environmental engineering, Brigham Young University, Provo, UT.

DEFLECTION AMPLIFICATION FACTORS FOR ESTIMATING INELASTIC DRIFTS

Roof Drifts

A typical response envelope of base shear ratio (C) versus lateral drift (Δ) is shown in Figure 3. In design, the inelastic roof drift of the system (Δ_m, in Figure 3) is estimated by multiplying the elastic drift (Δ_s) by a deflection amplification factor (DAF). The deflection amplification factor DAF is:

$$\text{DAF} = \mu_s \, \Omega \quad (1)$$

where $\mu_s = \Delta_m/\Delta_y$ and $\Omega = C_y/C_s$ (Uang, 1991; Uang and Maarouf, 1994). If the equal displacement principle holds true ($\Delta_e = \Delta_m$), the deflection amplification factor DAF should be equal to C_e/C_s, which is the strength reduction factor, R, used in design.

Previous studies indicate that low-rise structures require greater DAFs than high-rise structures. For low-rise structures that fall in the acceleration amplification region of the response spectra, Δ_m tends to exceed Δ_e (Newmark and Hall, 1982). Uang and Maarouf (1994) found that a DAF of 1.2 times the R factor (1.2R) was appropriate for a 2-story EBF with a ductility demand of 5. However, for three taller systems in that study (6- to 13-story steel and concrete moment frames), appropriate DAFs were in the range of 0.7 to 0.9R. Karavasilis et al. (2007) investigated X-braced steel frames and had similar results; back calculated DAFs were about 1.3 times the ductility demand for 3-story frames, but 0.6 to 0.8 times the ductility demand for 6- to 20-story frames.

Values of the deformation amplification factor, C_d, in current provisions reflect engineering judgment and compromise. The history of drift requirements and deformation amplifications factors is summarized by Searer and Freeman (2004). Current U.S. provisions (ICC, 2006) specify a deformation amplification factor, C_d, for EBFs of 4, which is 0.5 to 0.6 times the R factor. This value applies to all EBFs regardless of building height. The 1997 UBC (ICBO, 1997) specified a deflection amplification factor of 0.7R. Amplification factors in this range (0.5 to 0.7R) appear reasonable for mid- to high-rise structures based on the studies cited earlier, but seem too low to accurately predict inelastic roof drifts in low-rise buildings.

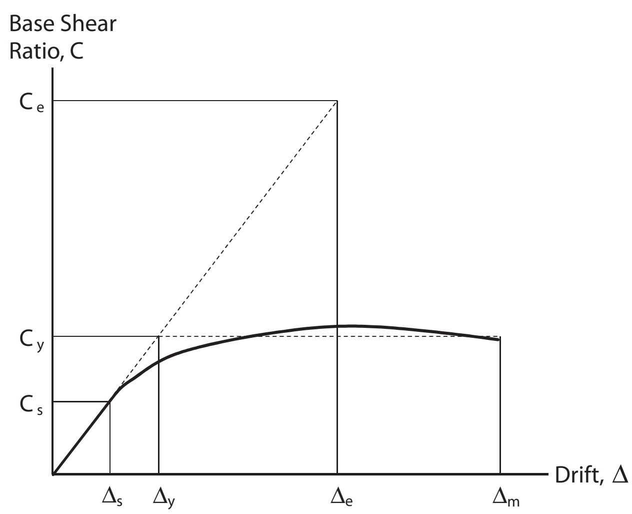

Fig. 3. General structural response envelope.

Story Drifts

The previous discussion on DAFs was in the context of predicting inelastic roof drifts. In practice, deformation amplification factors are commonly used for estimating inelastic story drifts because story drifts have prescribed limits (ICC, 2006). When the deformation amplification factors for roof drifts are extended directly to story drifts, the underlying assumption is that inelastic deformation is distributed evenly among the stories.

Because of weak stories, appropriate DAFs for predicting maximum story drifts are greater than those for predicting roof drifts. Uang and Maarouf (1994) found that deflection amplification factors to estimate maximum story drifts ranged from 1 to 1.5R for three buildings that had reasonable distribution of yielding, but was as high has 1.8R for a 6-story concrete building with a weak first story. In a much more exhaustive study of moment frames, Medina and Krawinkler (2005) found that maximum story drifts were 1.1 to 1.5 times the maximum roof drifts. This issue compounds the problems of using the current C_d factor to estimate story drifts in low-rise EBFs.

OBJECTIVE

This paper explores the accuracy of predicting EBF inelastic drifts and link rotations through amplification of elastic deformations. Inelastic drifts and rotations from nonlinear dynamic analyses of several EBFs are compared with those estimated by amplifying elastic deformations. Three approaches to developing better deformation amplification factors are investigated. Practical implications of the results are discussed and recommendations are made for improved EBF design.

EBF DESIGN AND ELASTIC DRIFTS

Design of Frames

Twelve EBF buildings were designed representing three heights (3-, 9-, and 18-story) and four strength levels. Building plan dimensions and floor masses matched those used in moment frame studies (Gupta and Krawinkler, 1999)

Table 1. Link Demand/Capacity Ratios and Frame Periods		
No. Stories	**Link D/C**	**Period (s)**
3	0.85	0.73
3	0.65	0.64
3	0.50	0.58
3	0.42	0.52
9	0.90	2.00
9	0.60	1.81
9	0.44	1.55
9	0.36	1.41
18	1.03	5.65
18	0.63	4.75
18	0.45	3.99
18	0.35	3.55

(see Figure 4). Seismic weights, W, for the 3-, 9-, and 18-story buildings were 7,160, 21,880, and 24,160 kips, respectively. Braced bays were located around the perimeter of the buildings. EBFs had two braces per bay. The 18-story buildings were 239 ft tall, just below the 240-ft maximum height allowed for braced frames (Seismic Design Category D, ICC, 2006).

Buildings were designed according to the 2006 IBC (ICC, 2006) equivalent lateral force procedure and AISC Seismic Provisions (2005). A Los Angeles, California, site was used for design with $S_{DS} = 1.11$ and $S_{D1} = 0.61$, where S_{DS} and S_{D1} are the site design spectral accelerations at 0.2 and 1.0 s in terms of gravity. S_{DS} and S_{D1} are based on the MCE × ⅔. The importance factor was taken as 1.0. The equivalent lateral forces for the 3-, 9-, and 18-story buildings were 0.134W, 0.056W, and 0.0342W, respectively.

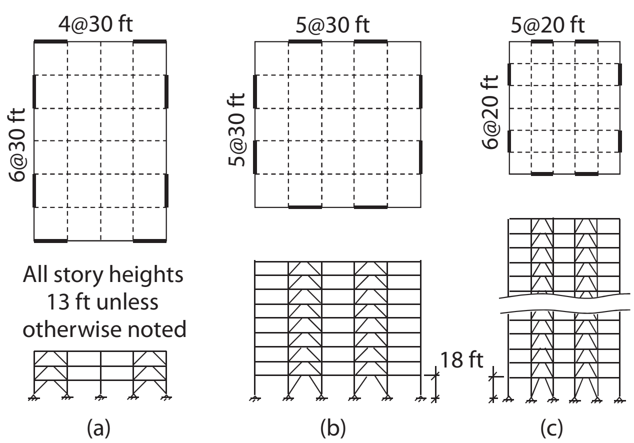

Fig. 4. Plan and elevation views of EBF buildings: (a) 3-story, (b) 9-story and (c) 18-story.

EBFs were designed for each of the buildings. To investigate the influence of strength, four designs were developed for each building height. For each design, a demand/capacity between 0.4 and 1.0 was selected for the links. Then links were sized to provide similar demand/capacity ratios at all floors (Popov et al., 1992). The average demand/capacity ratio (D/C ratio) for the links of each frame are indicated in Table 1. Frames with a D/C ratio relatively close to 1.0 represent typical designs, while those with a lower D/C are stronger than required to resist the equivalent lateral force. Member sizes for all frames can be found in Prinz (2007). As part of the design, elastic analysis under the equivalent lateral force was performed for each frame using the program RISA (RISA Technologies, 2005).

Elastic Drifts

Results from the elastic analyses provide some insight into the effect of frame strength on elastic story drifts. The elastic story drifts of each frame under the equivalent lateral force are shown in Figure 5. Total story drift is indicated with open squares, while solid squares indicate the component of the total drift caused by story shear distortion (Figure 2, middle). Equations for computing the story drifts components from model nodal displacements are developed in the Appendix. Frames with different D/C ratios had different member sizes and correspondingly different lateral stiffness. As frame stiffness increases (lower D/C ratios) elastic drifts decrease. Note that the shear component of the story drift is similar over the height each frame (Figure 5).

In Figure 5, a dashed line where drift equals 0.005 indicates an elastic story drift that will result in an estimated inelastic drift of 0.02 (4 × 0.005), which is the inelastic story drift limit for these frames. The 9-story frame with D/C = 0.90 and all of the 18-story frames have noncompliant story drifts in upper stories when typical procedures are used to estimate inelastic drift.

ADDITIONAL MODELING AND ANALYSIS

Techniques

Individual frames were modeled as two-dimensional systems using the nonlinear dynamic analysis program Ruaumoko (Carr, 2006). Standard beam elements with bilinear flexural-axial hinges at each end were used to represent beams and columns. Links were modeled with beam elements and springs in an arrangement that has been used and validated in previous EBF studies (Richards and Uang, 2006; Ramadan and Ghobarah, 1995). Columns at the base of the frames were considered fixed. Beam-column connections were considered rigid when a gusset plate would be present and pinned when not present.

Expected material strengths were specified for the ductile elements in the models, while nominal strengths were used for other members. EBF shear link elements had maximum strengths of $1.55V_n$ ($R_y = 1.1$, $\omega = 1.41$) based on experimental data for ASTM A992 shear links (Okazaki et al., 2005), where V_n is the nominal shear capacity of the link, R_y is the ratio between expected and nominal material strength, and ω is the strain hardening factor.

A single continuous column in each model represented all the gravity columns associated with the frame (one-fourth of the building). This representative column had stiffness and strength at each story corresponding to the sum of the gravity columns, assuming weak axis bending. Gravity loads corresponding to $1.2D + 0.5L$ (ICC, 2006) were applied to this column during the analyses, where D and L are dead and live load effects. This column was pinned at the base and constrained to match the frame displacements at each floor level.

Analyses

Modal and pushover analyses were performed for model characterization. The pushover analyses used the lateral force distribution prescribed by the equivalent lateral force procedure (ICC, 2006).

Dynamic analyses were performed using suites of ten earthquake records, primarily from California events (Tables 2 and 3). Earthquake records were scaled so that the mean spectral acceleration of the suite for a range of building periods was greater than the design spectra over the same range. Compared to period-independent scaling procedures, this method of scaling has been shown to result in reduced scatter of response data (Kurama and Farrow, 2003). The mean spectra of the scaled records are shown in Figure 6 with the design spectra. Different suites were used for the analysis of the 3- and 9-story and the 18-story frames (Tables 2 and 3) so that scaling factors greater than 3 were not required.

Rayleigh damping was used in the dynamic analyses with consideration of its potential problems. Ricles and Popov (1994) and Hall (2005) have demonstrated that Rayleigh damping may result in unrealistically high damping forces during time history analyses for some cases. To investigate the sensitivity of final results to damping assumptions, analyses were performed twice, first with 2% Rayleigh damping specified at the fundamental period and at a period of 0.2 s, and again with 0.5% damping specified at the same periods.

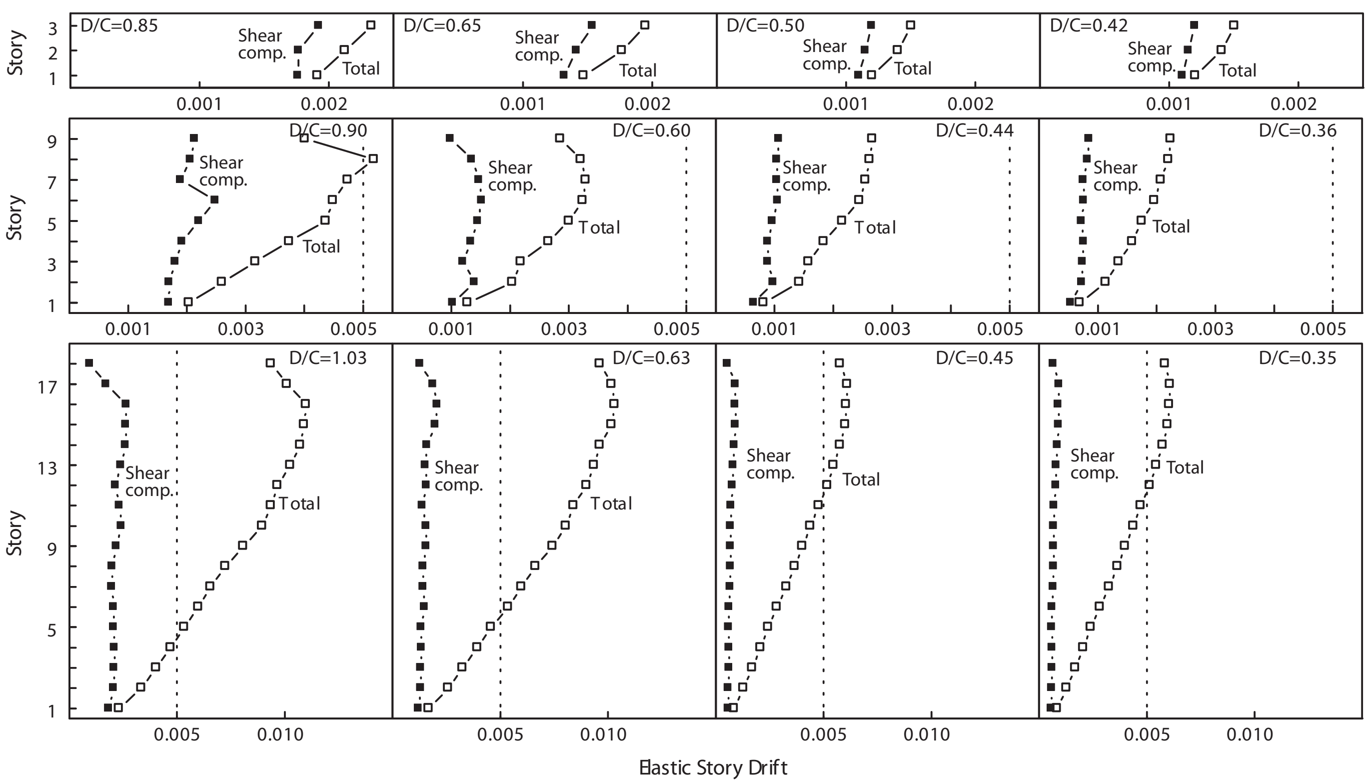

Fig. 5. Elastic story drifts under the equivalent lateral force.

Table 2. Earthquake Records Used for 3- and 9-Story Frame Analyses

Record	PGA[a] (g)	R[b] (km)	Site[c]	Scale Factor
1994 Northridge				
Canoga Park, NORTHR/CNP196[d]	0.42	15.8	D	2.06
90013 Beverly Hills, NORTHR/MUL279	0.52	19.6	C	1.07
90018 Hollywood, NORTHR/WIL180	0.25	25.7	C	1.85
90006 Sun Valley, NORTHR/RO3090	0.44	12.3	D	1.27
1989 Loma Prieta				
1656 Hollister Array, LOMAP/HDA255	0.28	25.8	D	2.20
Hollister City Hall, LOMAP/HCH180	0.22	28.2	D	1.54
Gilroy No. 3, LOMAP/GO3090	0.37	14.4	D	2.60
Gilroy No. 4, LOMAP/GO4090	0.21	16.1	D	2.53
1987 Superstition Hills				
Parachute Test Site, SUPERST/B-PTS225	0.46	0.7	C	1.02
Parachute Test Site, SUPERST/B-PTS315	0.38	0.7	C	2.02

a. Peak Ground Acceleration
b. Distance to fault rupture
c. NEHRP Site class
d. Designation in Pacific Earthquake Engineering Research (PEER) database

Table 3. Earthquake Records Used for 18-Story Frame Analyses

Record	PGA[a] (g)	R[b] (km)	Site[c]	Scale Factor
1999 Duzce, Turkey				
Duzce, DUSCE/DZC270[d]	0.54	8.2	D	0.86
1999 Chi-Chi, Taiwan				
TCU063, CHICHI/TCU063-N	0.13	10.4	D	0.90
CHY101, CHICHI/CHY101-N	0.44	11.4	D	0.59
1999 Kocaeli, Turkey				
Yarimca, KOCAILI/YPT060	0.27	2.6	D	0.83
Yarimca, KOCAILI/YPT330	0.35	2.6	D	0.97
1994 Northridge				
90056 Newhall, NORTHR/WPI046	0.46	7.1	C	1.28
1992 Landers				
24 Lucerne, LANDERS/LCN275	0.72	1.1	B	0.71
1979 Imperial Valley				
955 El Centro Array #4, IMPVALL/H-E04230	0.36	4.2	D	0.87
952 El Centro Array #5, IMPVALL/H-E05230	0.38	1.0	D	0.82
942 El Centro Array #6, IMPVALL/H-E06230	0.44	1.0	D	0.70

a. Peak Ground Acceleration
b. Distance to fault rupture
c. NEHRP Site class
d. Designation in Pacific Earthquake Engineering Research (PEER) database

Model Characterization

Results from the modal and pushover analyses provide a reasonable level of confidence in the designs and the models. The natural period of each frame is shown in Table 1 (last column). The approximate fundamental periods given by design provisions are 0.66, 1.41, and 2.55 s for the 3-, 9-, and 18-story frames, respectively (ICC, 2006). As expected, the natural period of the model frames are close-to or greater than the approximate periods. Results from the pushover analyses are given in Figure 7. The drift at yield is similar for all frames of a given geometry, despite large differences in strength.

RESULTS FROM NONLINEAR DYNAMIC ANALYSES

Damping

Drifts from the analyses with 2% damping will be discussed in the remainder of the paper. Compared with the models with 0.5% damping, the models with 2% damping had lower story drifts (around 20% lower for most stories, but as low as 50%), but greater maximum brace and column demands (around 5% greater for most columns, but as much as 10% greater). This is because relatively high link rotation velocities generate large damping forces, unrealistically increasing brace and column demands (Ricles and Popov, 1994). While 2% viscous damping may result in excess brace and column forces, it is believed to provide reasonable values for drifts (and link rotations).

Inelastic Roof Drifts

Roof drifts were computed using data from the nonlinear dynamic and static elastic analyses. For each frame, the roof drift from the dynamic analyses is the average of the maximum roof drift that occurred under each of the ten records. Average values are used since more than seven records were considered (ICC, 2006). The amplified elastic roof drift is the roof drift from the elastic analysis under the equivalent lateral force multiplied by the factor C_d/I. C_d/I was equal to 4.0 for all frames.

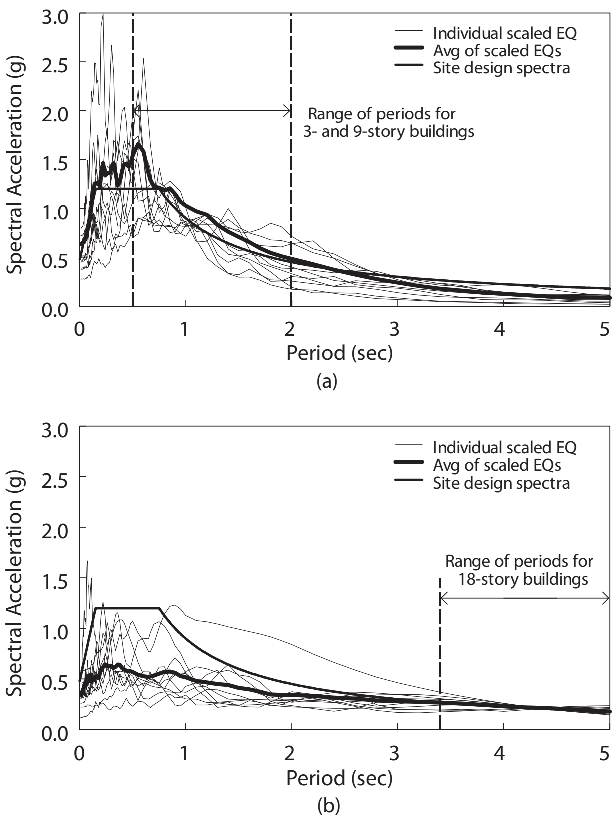

Fig. 6. Response spectra of earthquakes scaled for (a) 3- and 9-story buildings and (b) 18-story buildings.

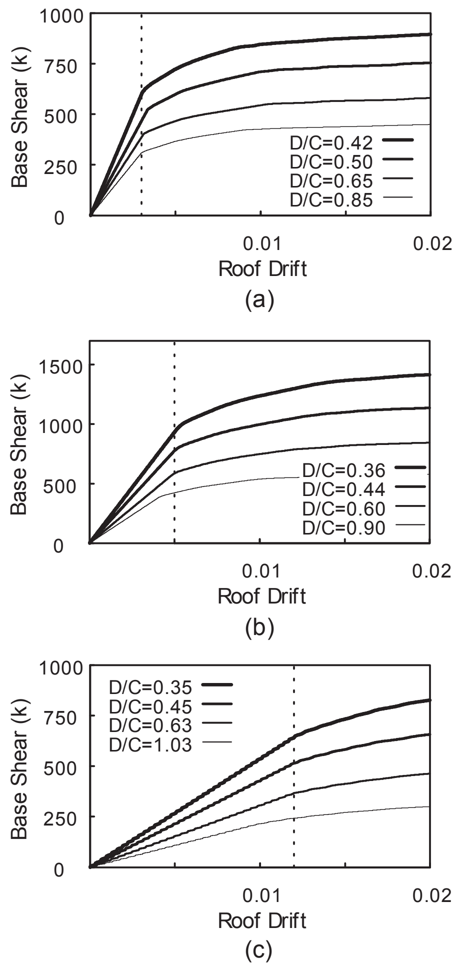

Fig. 7. Pushover analysis results: (a) 3-story, (b) 9-story and (c) 18-story.

Short and tall frames have different relationships between strength and roof drift. Figure 8 shows roof drift as a function of frame strength (D/C ratio) for the 3-, 9-, and 18-story frames. For the 3-story frames, there is an increase in roof drift as frame strength decreases (D/C ratio increases) (Figure 8). However, for the 9- and 18-story frames, roof drifts from the dynamic analyses are largely independent of frame strength. Estimating roof drifts by amplifying elastic drifts by a factor of 4.0 is somewhat unconservative for short frames and overly conservative for tall frames with D/C ratios near 1.0. This observation is consistent with the other studies that were discussed previously.

Inelastic Story Drifts

Story drifts were computed using data from the nonlinear dynamic and the linear static analyses (see Appendix). Story drifts from the dynamic analyses were computed as the average of the maximum story drifts for each floor from ten analyses (circles in Figure 9). Story drifts were estimated from the elastic analyses by amplifying the elastic story drifts by the factor C_d/I (triangles in Figure 9).

Maximum story drifts from the dynamic analyses occurred in the lower story of the 3-story frames (Figure 9, top row), and in the top few stories of the 9- and 18-story

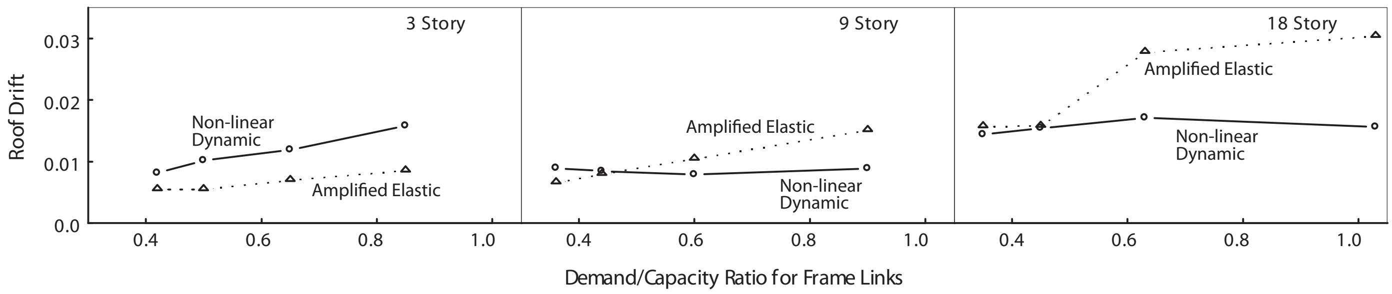

Fig. 8. Roof drifts computed from analyses.

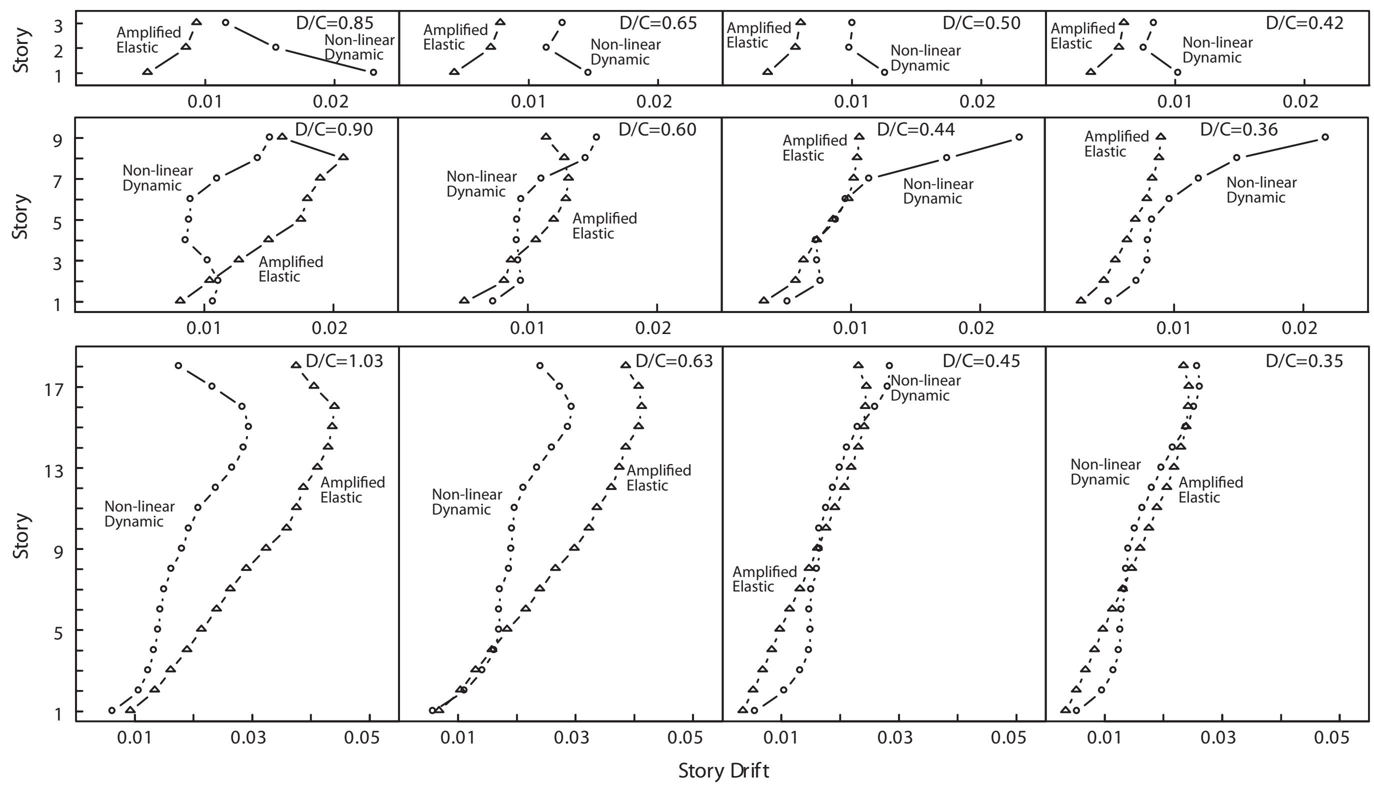

Fig. 9. Story drifts computed from analyses.

frames (Figure 9, middle and bottom rows). For the 3-story frames, the maximum story drift decreases as frame strength increases (D/C decreases); however, in the 9-story frames, the story drifts at the top of the frames increase as frame strength increases. It appears that reduced yielding at the base of the 9-story frames resulted in greater response in the upper stories. For the 18-story frames, maximum story drifts are similar for all D/C ratios.

Correlation between the amplified elastic story drifts and the dynamic analyses drifts improves as D/C ratios decrease. Considering Figure 9, correlation is quite poor for frames with D/C ratios closer to 1.0 (left side) but improves, and might be considered good, for taller frames with low D/C ratios (right side). This is because the stronger frames experience more of a first mode elastic response, giving a distribution of drifts more similar to the elastic analysis. Unfortunately, typical designs have D/C ratios closer to 1.0, placing them in the region of poor correlation. For the 3-story frames with D/C = 0.85, the amplified static drift at the first story was only 26% of that observed in the dynamic analyses (Figure 9). For the 9- and 18-story frames reasonable correlation was observed in the bottom stories; however, drifts in the upper stories from amplified elastic drifts were nearly two times the drifts from the dynamic analyses for 18-story frames with D/C close to 1.0.

Additional insights into the behavior of the frames can be gained by considering the portion of the drifts coming from story shear deformations. Figure 10 indicates the shear component of the maximum story drifts from the dynamic analyses with solid circles. The open circles are the total drift and have the same values as in Figure 10. For the 3- and 9-story frames, the majority of the drift for all stories is from story shear deformations; for the 18 story frame with D/C = 1.03, shear deformations account for at least half of the story drift for most stories. As might be expected, the percentage of drift from shear deformations in taller frames is much greater than that given by elastic analysis (compare Figure 10 and Figure 5).

Inelastic Link Rotation

Link rotations were computed using data from the nonlinear dynamic and the static elastic analyses (see Appendix). Link rotations from the dynamic analyses were computed as the average of the maximum link rotations for each floor from ten analyses (circles in Figure 11). Link rotations were estimated from the elastic analyses by multiplying the elastic story drifts by C_d/I to get an estimated inelastic drift and then multiplying that by L/e (see Figure 1).

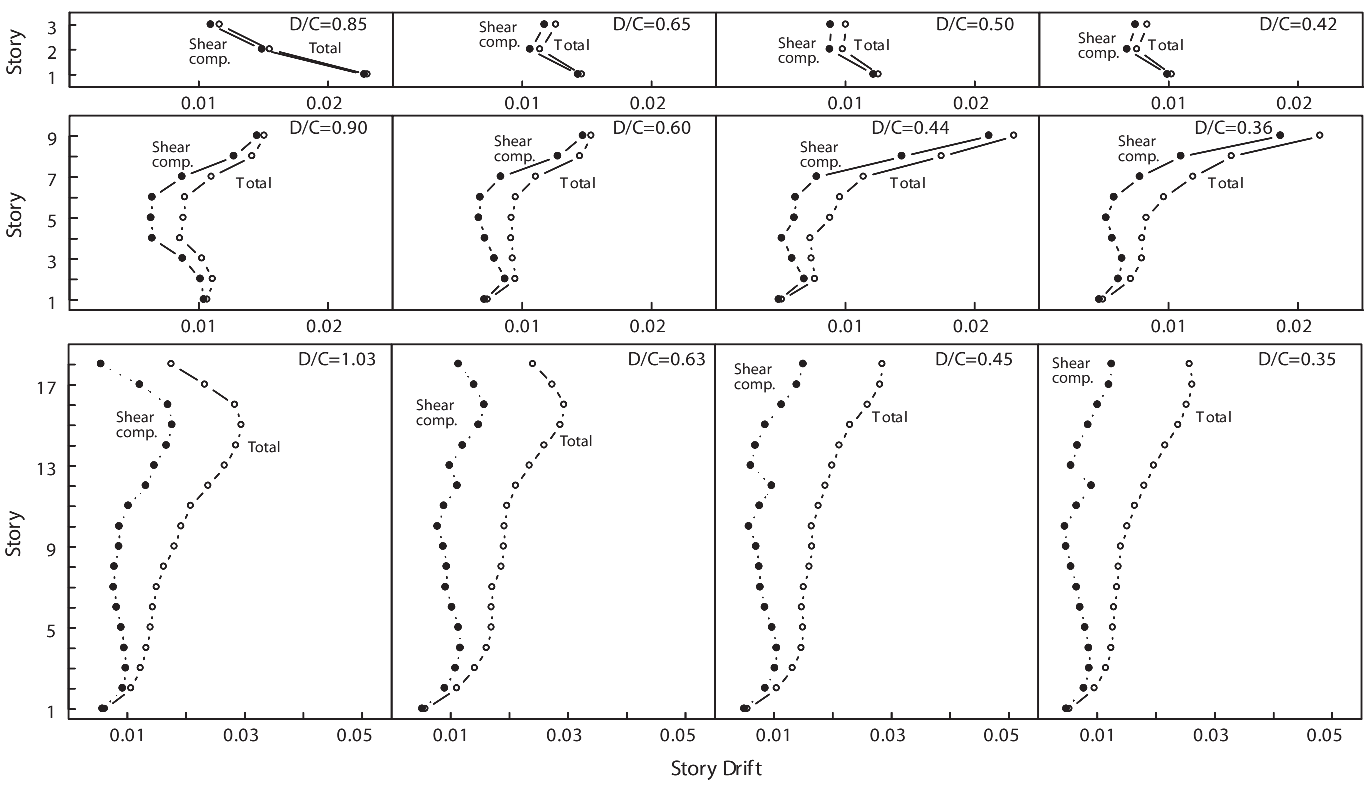

Fig. 10. Comparing shear component of story drift with the total story drift from dynamic analyses.

For most of the frames, the differences between the dynamic and amplified elastic values of link rotation are similar to the differences in story drifts (compare Figure 11 and Figure 9). When link lengths are the same at each floor, the relationship assumed by Figure 1 scales all of the drifts from Figure 9 by the same value. The greatest discrepancy between Figure 11 and Figure 9 is for stories in frames where the majority of the drift is not from shear deformations. For typical frames (with D/C near 1.0) the amplified elastic estimates of link rotation do not correspond well to those from the dynamic analyses; estimates are too low for the 3-story frames and too high for the others.

ALTERNATIVE METHODS OF ESTIMATING LINK INELASTIC ROTATION

Since the current approach for estimating link rotations appears inaccurate, three alternative methods for estimating link inelastic rotation were explored. The first is using a calibrated story-specific C_d factor to scale total elastic story drifts, and then compute link rotation using Figure 1. The second method is using a calibrated story-specific C_d factor to scale the shear component of story drift, and then compute link rotation using Figure 1. The third method is using a story-specific rotation amplification factor to scale elastic link rotations directly to yield inelastic link rotations.

Method 1

A calibrated deformation amplification factor can be computed by combining results from the nonlinear dynamic analyses with the static elastic analyses. The typical method of estimating link rotation is:

$$(\text{elastic drift}) \times C_d \times (L/e) = (\text{inelastic link rotation}) \qquad (2)$$

where C_d is constant. Analysis results were used to solve for C_d for each story of each frame given the elastic drift from the elastic analyses, and the inelastic link rotation from the dynamic analyses:

$$C_{d,\,calib} = (\text{inelastic link rotation})/[(\text{elastic drift}) \times (L/e)] \qquad (3)$$

The computed values of $C_{d,\,calib}$ are indicated in Figure 12(a). A value of 4.0 (currently used for design) is indicated by a dashed line in Figure 12(a).

From Figure 12(a) it is clear that no single value of C_d will give a reasonable estimate of link rotation for all stories of all frames. The present value of 4.0 gives reasonable

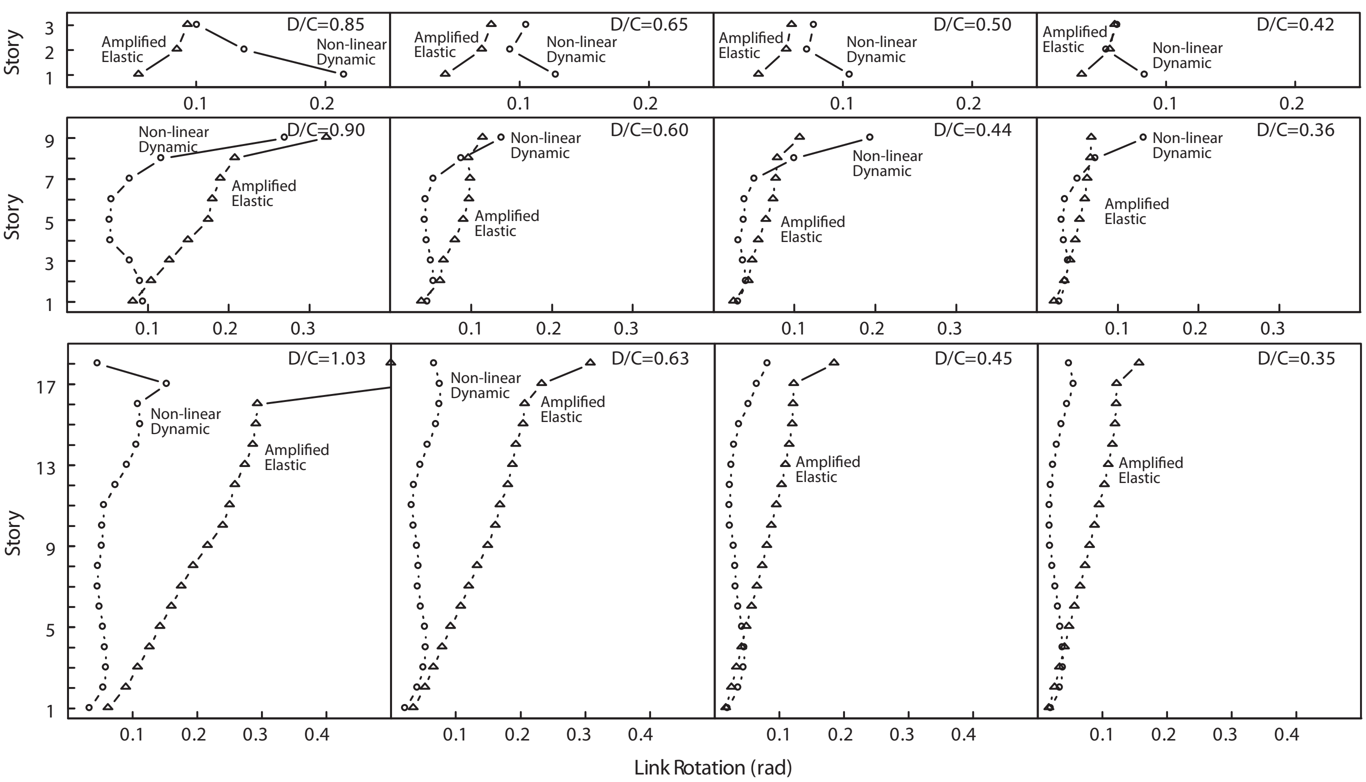

Fig. 11. Link rotations computed from analyses.

estimates of link rotations in the top two stories of the 3-story frames and in the bottom stories of the 9-story frames.

The grouping for the 9-story frames in Figure 12(a) gives a sense of the sensitivity of the results to frame geometry. The 9-story frame with D/C = 0.90 had links that were 3 ft long (except the top story), while the other 9-story frames had links that were 4 ft long (except top story). The frame with D/C = 0.90 has similar calibrated C_d factors as compared to the others, but it appears there is some sensitivity of the result to geometry. For the 3- and 18-story frames, similar link sizes were used for frames of all D/C ratios (except in the top stories of the 18-story frames), so differences in $C_{d,\ calib}$ are entirely due to strength.

Method 2

Another type of deformation amplification factor can be developed that scales only the shear component of the elastic story drift. This factor is computed as:

$$C_{d,\ shear} = \text{(inelastic link rotation)} / [\text{(shear component of elastic drift)} \times (L/e)]. \quad (4)$$

The computed values of $C_{d,\ shear}$ are indicated in Figure 12(b). In comparing Figure 12(b) with Figure 12(a), specifically the taller frames with the highest D/C ratios, values of $C_{d,\ shear}$ appear to have better vertical alignment than $C_{d,\ calib}$, making them better suited to be represented by a constant value. For example, a constant value of 5.0 for $C_{d,\ shear}$ might give a reasonably conservative estimate for link rotations for the 9- and 18-story frames of this study. Refer to Figure 4 and Prinz (2007) for the specific geometry and sizes for the frames that these factors are based on; in general, bay widths were 20 to 30 ft, bay heights were 13 ft, and link lengths were 3 to 4 ft.

Method 3

The third type of factor considered was a link rotation amplification factor (RAF) that would provide a direct estimation of link inelastic rotation from the link rotation of the elastic analysis. This factor, RAF was computed from the data as:

$$\text{RAF} = \text{(inelastic link rotation)/(elastic link rotation)} \quad (5)$$

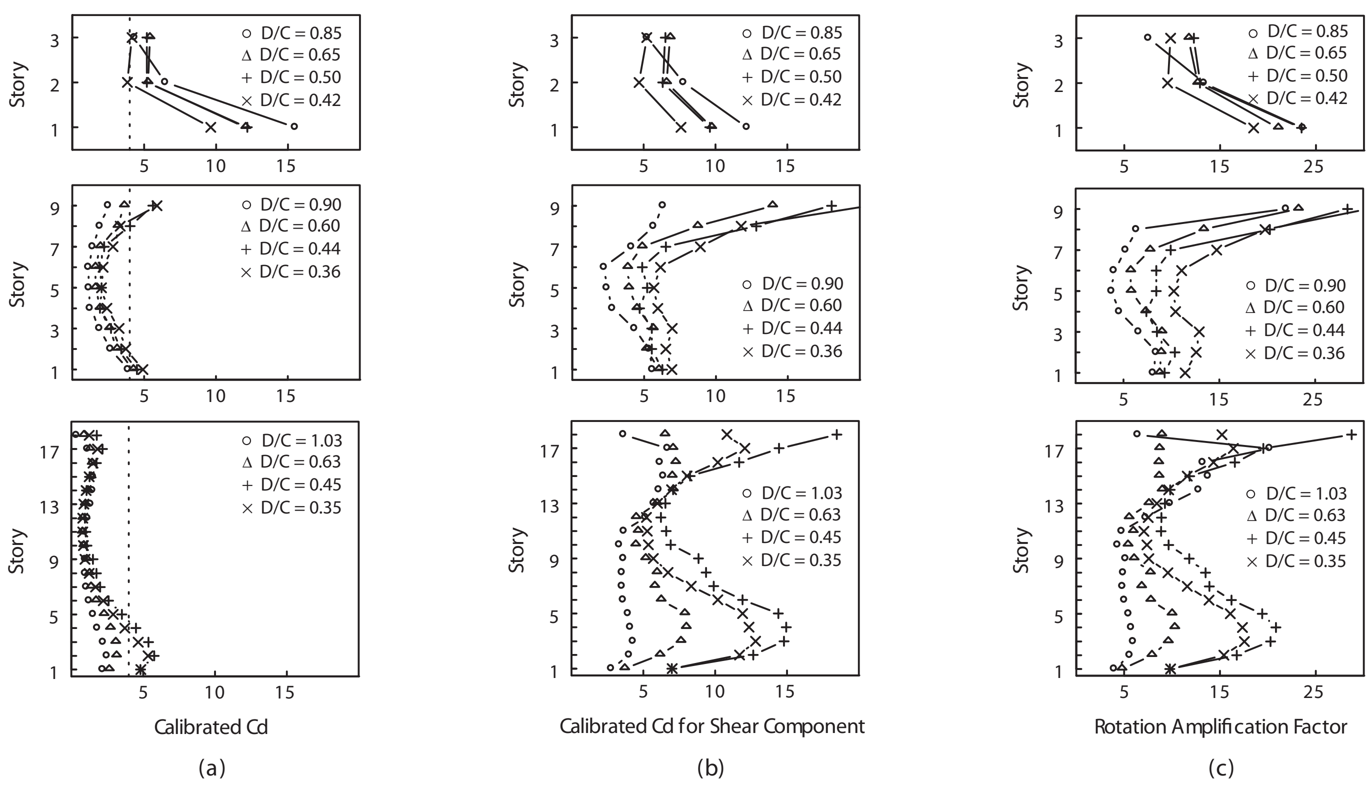

Fig. 12. Amplification factors for estimating inelastic deformations: (a) $C_{d,\ calib}$ *for estimating link rotations using total elastic story drift, (b)* $C_{d,\ shear}$ *for estimating link rotations using the shear component of the elastic story drift, and (c) rotation amplification factor for estimating inelastic link rotations using elastic link rotations.*

where inelastic link rotation came from the dynamic analyses. Values for the RAF are given in Figure 12(c). Values for this factor are less tightly grouped and appear more sensitive to frame strength. There appears to be no benefit to using the RAF instead of the $C_{d,\ shear}$.

SUMMARY AND PRACTICAL IMPLICATIONS

The ductility of steel eccentrically braced frames (EBFs) depends on stable inelastic rotation of the links. Links are sized and detailed so that inelastic rotation demands do not exceed inelastic rotation capacities. Typically, design engineers amplify elastic analysis results to estimate EBF link inelastic rotations. In this study, twelve EBFs (3-, 9-, and 18-story) were designed and investigated using time history analyses. Roof drifts, story drifts, and link rotations obtained from the time history analyses were compared with those estimated by amplifying elastic analysis results. In general, poor correlation was observed for most stories in typical frames. Three other methods for estimating inelastic link rotations were considered.

Low-rise EBFs will experience greater story drifts and link rotations than predicted by amplified elastic analysis. The value of the deformation amplification factor, C_d, is too low to accurately estimate inelastic drifts in low-rise buildings. Since inelastic drifts are underestimated, inelastic link rotations are also underestimated. Designers should keep this in mind when sizing links and determining appropriate stiffeners in low-rise buildings.

Mid to high-rise EBFs will experience much lower story drifts and link rotations than predicted by amplified elastic analysis. This is primarily due to the fact that elastic drifts which include the flexural component caused by column elongation are amplified.

Calibrated C_d factors are necessary for designers to reasonably estimate inelastic drifts and link rotations in EBFs. Results indicate that using a constant factor to scale the elastic shear deformation will yield more reasonable results for taller buildings than the present method of scaling total deformation. A factor of 5.0 was reasonable for the 9- and 18-story frames in this study with D/C near 1.0. The frames considered in the study had 20- to 30-ft bay widths, 13-ft typical bay heights, and link lengths of 3 to 4 ft. It appears the calibrated C_d factors are somewhat sensitive to EBF geometry, so this study is inadequate to recommend factors for general design.

ACKNOWLEDGMENTS

This work was possible due to the support of Brigham Young University. Matt Merrell, former student at Brigham Young University, assisted in the design of the frames used in the study. Reviewers provided helpful suggestions that significantly improved the paper. Their contribution is appreciated by the authors.

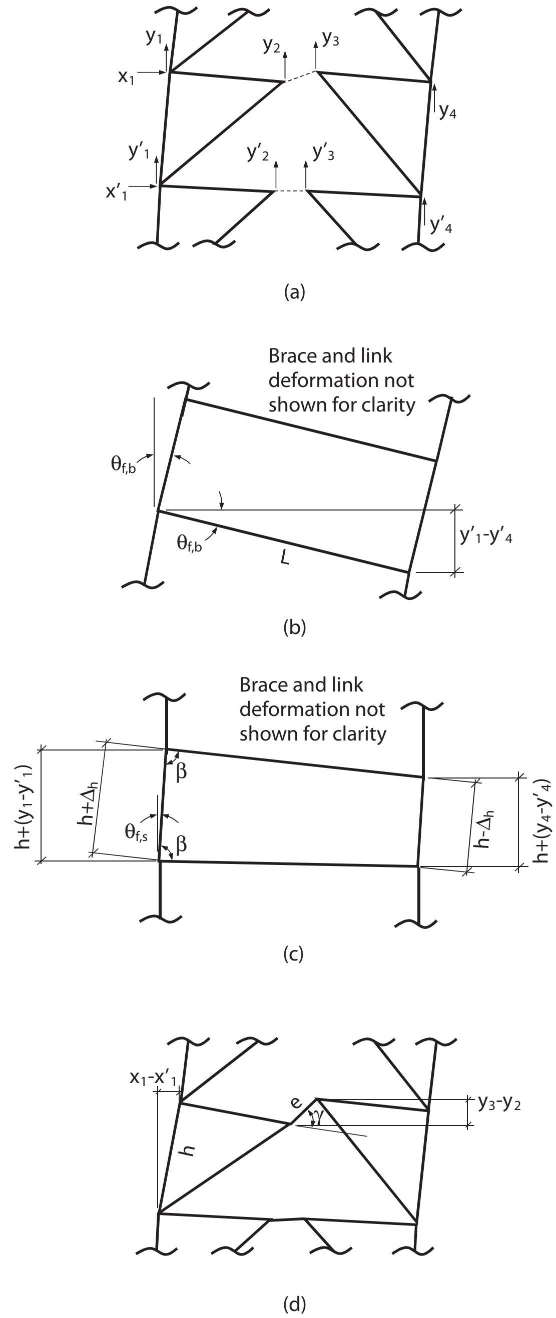

Fig. 13. Computing drift components and link rotations: (a) nodal displacements used for calculations; (b) component of story drift due to axial deformations in columns below; (c) component of story drift due to axial deformation in columns of story; (d) geometry for computing link rotations.

APPENDIX

Total story drifts and drift components were computed using nodal displacements from the analysis outputs. The six nodal displacements required to compute the components of drift for a story are x_1, y_1, y_4, x'_1, y'_1 and y'_4, as defined in Figure 13(a).

The total story drift, as defined by current provisions (ICC 2006), is:

$$\theta_T = (x_1 - x'_1)/h \tag{6}$$

where h is the story height. One component of this total story drift, is due to column shortening or elongation in the stories below, $\theta_{f,b}$. From the geometry shown in Figure 13(b), $\theta_{f,b}$ is:

$$\theta_{f,b} = \arcsin[(y'_1 - y'_4)/L] \tag{7}$$

Another component of the total story drift comes from column shortening or elongation in the story in question, $\theta_{f,s}$ [illustrated in Figure 13(c)]. From the geometry of Figure 13(c), $\theta_{f,s}$ is:

$$\theta_{f,s} = 90° - \beta \tag{8}$$

where

$$\beta = \arccos(\Delta_h/L) \tag{9}$$

From similar triangles in Figure 13(c),

$$(h + \Delta_h)/[h + (y_1 - y'_1)] = (h - \Delta_h)/[h + (y_4 - y'_4)] \tag{10}$$

which can be solved for Δ_h:

$$\Delta_h = h(R - 1)/(R + 1) \tag{11}$$

where

$$R = [h + (y_1 - y'_1)]/\ [h + (y_4 - y'_4)] \tag{12}$$

Combining Equations 10 to 14, $\theta_{f,s}$ can be expressed in terms of nodal displacements:

$$\theta_{f,s} = 90° - \arccos\{[h(R - 1)]/[L(R + 1)]\} \tag{13}$$

Finally, the shear component of the total story drift, θ_s, is:

$$\theta_s = \theta_T - \theta_{f,b} - \theta_{f,s} \tag{14}$$

Link rotation, γ, was computed using nodal displacements x_1, x'_1, y_2 and y_3. From Figure 13(d) the relationship is:

$$\gamma = (y_3 - y_2)/e + (x_1 - x'_1)/h \tag{15}$$

REFERENCES

AISC (2005), *Seismic Provisions for Structural Steel Buildings*, American Institute of Steel Construction, Inc., Chicago.

Carr, A. (2004), *Ruaumoko Users Manual*, University of Canterbury, Christchurch, New Zealand.

Gupta, A. and Krawinkler, H. (1999), "Prediction of Seismic Demands for SMRFs with Ductile Connections and Elements," *Report SAC/BD-99/06*, SAC Joint Venture, Sacramento, CA.

Hall, J. (2005), "Problems Encountered from the Use (or misuse) of Rayleigh Damping," *Earthquake Engineering and Structural Dynamics*, Vol. 35, No. 5, 525–545.

Horne, J.P., Rubbo, A. and Malley, J.O. (2001), "AISC-LRFD Design and Optimization of Steel Eccentrically Braced Frames," *Proceedings of 70th Annual SEAOC Meeting*, San Diego, CA.

International Code Council (ICC) (2006), *International Building Code*, International Code Council, Inc., Whittier, CA.

International Conference Building Officials (ICBO) (1997), *Uniform Building Code*, International Conference Building Officials, Whittier, CA.

Karavasilis, T.L., Bazeos, N. and Beskos, D.E. (2007), "Estimation of Seismic Drift and Ductility Demands in Planar Regular X-Braced Steel Frames," *Earthquake Engineering and Structural Dynamics*, Vol. 36, No. 15, 2273–2289.

Kurama, Y.C. and Farrow, K.T. (2003), "Ground Motion Scaling Methods for Different Site Conditions and Structural Characteristics," *Earthquake Engineering and Structural Dynamics*, Vol. 32, No. 15, 2425–2450.

Medina, R.A. and Krawinkler, H. (2005), "Evaluation of Drift Demands for the Seismic Performance Assessment of Frames," *Journal of Structural Engineering*, Vol. 131, No. 7, 1003–1013.

Newmark, N.M. and Hall, W.J. (1982), *Earthquake Spectra and Design*, Earthquake Engineering Research Institute, El Cerrito, CA.

Okazaki, T., Arce, G., Ryu, H.-C. and Engelhardt, M.D. (2005), "Experimental Study of Local Buckling, Overstrength, and Fracture of Links in Eccentrically Braced Frames," *Journal of Structural Engineering*, Vol. 131, No. 10, 1526–1535.

Popov, E.P., Ricles, J.M. and Kasai, K. (1992), "Methodology for Optimum EBF Link Design," *Proceedings of the 10th World Conference on Earthquake Engineering*, Balkema, Rotterdam, Vol. 7, 3983–3988.

Prinz, G. (2007). *Impact of Beam Splicing on Seismic Response of Buckling Restrained Braced Frames, Masters Thesis* (advisor: P. Richards), Brigham Young University, Provo, UT.

Ramadan, T. and Ghobarah, A. (1995), "Analytical Model for Shear-Link Behavior," *Journal of Structural Engineering*, Vol. 121, No. 11, 1574–1580.

Richards, P. and Uang, C-M. (2006), "Testing Protocol for Short Links in Eccentrically Braced Frames," *Journal of Structural Engineering*, Vol. 132, No. 8, 1183–1191.

Ricles, J.M. and Popov, E.P. (1994), "Inelastic Link Element for EBF Seismic Analysis," *Journal of Structural Engineering*, Vol. 120, No. 2, 441–463.

RISA Technologies (2005), *RISA-2D Version 6.0 User's Guide*, Foothill Ranch, CA.

Roeder, C.W. and Popov, E.P (1978), "Eccentrically Braced Steel Frames for Earthquakes," *Journal of the Structural Division*, Vol. 104, No. ST3, 391–412.

Searer, G.R. and Freeman, S.A. (2004). "Design Drift Requirements for Long-Period Structures," *Proceedings of the 13th World Conference on Earthquake Engineering*, Vancouver, B.C. Canada.

Uang, C.-M. (1991). "Establishing R (or R_w) and C_d Factors for Building Seismic Provisions," *Journal of Structural Engineering* Vol. 117, No. 1, 19–28.

Uang, C.-M. and Maarouf, A. (1994), "Deflection Amplification Factor for Seismic Design Provisions," *Journal of Structural Engineering,* Vol. 120, No. 8, 2423–2436.